Simultaneous T2 and T2* dynamic susceptibility contrast perfusion imaging using a multi-echo parallel imaging approach

R. D. Newbould[1], S. Skare[1], G. Albers[2], and R. Bammer[1]

[1]Radiology, Stanford University, Stanford, CA, United States, [2]Stanford Stroke Center, Stanford University, Stanford, CA, United States

Introduction. The utility of multi-echo DSC with gradient echo (GRE) EPI[1] has recently been demonstrated for improved AIF determination, T1 independent contrast concentration estimation, and SNR recovery. In order to quantify the difference between the static and dynamic dephasing regimes, a gradient and spin echo (GRASE) multi-shot multi-echo EPI sequence is demonstrated. The hemodynamic parameters determined by the GRE images are weighted towards the large vessels, while the SE images are more sensitive to the microvasculature. Further, the ratio of T2 to T2* may be indicative of mean vessel size in the voxel[2]. One group previously used alternating GE and SE EPI scans[3] as well as an early GRE readout and very late SE (110ms) readout from the same excitation[4]. Here, the reduced readout lengths not only improve EPI image quality, but allow several GRE readouts before a SE readout of similar TE as commonly used (75ms) for bolus tracking.

Aside from the geometric distortions and poor resolution associated with EPI scans, the contrast agent passage in DSC increases EPI image artifacts[5]. There can be profound problems accurately determining an arterial input function (AIF), which is necessary to obtain the tissue residue function by deconvolution[6] and consequently affects the veracity of the hemodynamic parameters. Image quality issues arise mainly due to (i) strong T2*-induced blurring, (ii) susceptibility gradients emanating from the sinuses and the auditory canals adjacent to the brain, (iii) susceptibility gradients between the high-concentration feeding vessels and the surrounding tissue, and (iv) the high concentration of contrast material in the vessels during bolus passage that causes clipping of the bolus maximum for typical echo times. The determination of the AIF from a magnitude weighted fit of the gradient echoes has been shown to be robust against vessel susceptibility shifts and signal saturation[5].

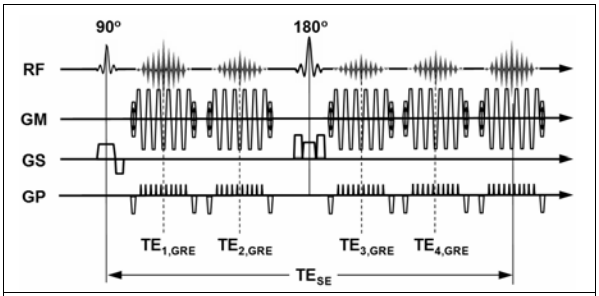

Figure 1. Pulse sequence diagram. Using parallel imaging the shortened EPI readouts allow multiple acquisitions during the FID for dynamic sampling of ΔR2* by several GRE's. ΔR2 information is collected by the SE. The GRE readouts are placed asymmetrically about the 180 pulse.

Here, a multi-shot interleaved EPI acquisition with self-calibrated PI is used to restore temporal resolution back to that of each interleaf for the high temporal localization needed in DSC. The shortened readouts, aside from improving EPI image quality, allow the collection of multiple echoes before the commonly used echo time in DSC. In this work, a SE readout is placed at a defined TE, and as many gradient echoes as allowed by resolution, slew rate, and interleaving are placed in the otherwise unused time between excitation and the SE (Fig 1). As the 180° pulse reverses the deterministic phase accumulation, GRE readouts are placed asymmetrically about the 180 pulse.

Materials and Methods. A multi-slice multi-echo DSC-PWI pulse sequence was developed for a 1.5T scanner (GE Signa LX, 12.0, grads=50 mT/m, *SR*=150) with interleaved multi-shot echo-planar readouts (Fig 1). Each interleaf was reconstructed separately using a GRAPPA based algorithm where weights were determined by combining all interleaves of the first echo (which has the highest SNR) to a fully sampled *k*-space. Each shot for each echo and slice in the TR thus forms a full image, with reduced distortions and blur. The GREs allow calculation of ΔT2* on a per pixel basis by means of a magnitude weighted non-linear fit, while the SEs are used for a ΔT2 calculation. Informed volunteer imaging was obtained using a dedicated 8-channel head coil (MRI Devices: *FOV*=24cm; *slice/gap*=5/1mm; *slices*=12; *TR*=1.125ms; matrix 96×96; α=70°; NEX=1; timepoints=60). A 3-interleaved EPI train acquired 2 GRE's (15.3 and 51.1 ms) and 1 SE (75ms) per excitation. After 15s of baseline scans, 17ml Multihance (Bracco, Princeton, NJ) (0.15mmol/kg BW) was injected at a rate of 6ml/s followed by a 20ml saline flush using a dual-piston power injector (Spectris, Medrad, Indianola, PA). A total of 2160 images were acquired in 76s with temporal resolution of 1.225s.

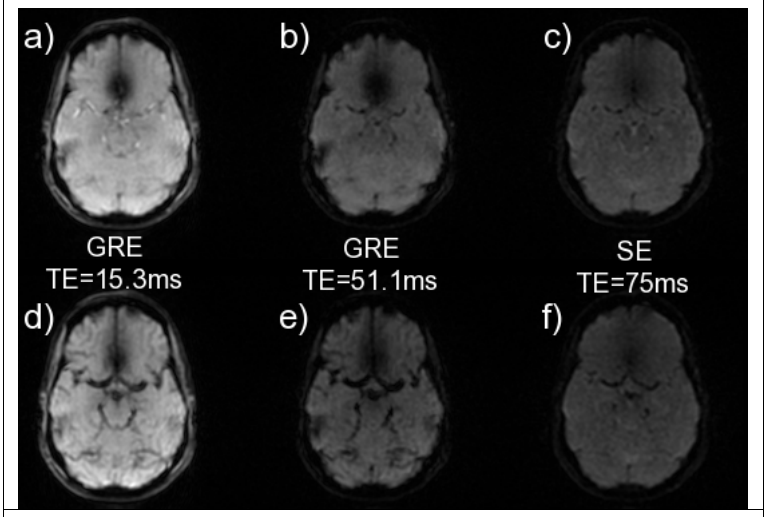

Figure 2. Raw images at the MCA level for baseline [a) - c)] and bolus peak [d) - f)] timepoints. Note the vessel blooming on the GRE images.

Results. Initial volunteer imaging is presented in Figure 2. Two GRE images and one SE image are shown for a slice from a volume before the bolus passage (top row) and during the bolus peak (bottom row). The early GREs are ideal for determining an AIF, due to the high contrast material concentration. The SE images do not exhibit the vessel blooming seen on both earlier GRE images, but rather a more diffuse lowered intensity from the contrast material's presence in the microvasculature.

Conclusion. The use of T2 vs. T2* contrast for DSC elucidates the physiological function differently. While GRE is weighted heavily by the large feeding vessels, SE reflects the microvasculature. The determination of an AIF is more straightforward with GRE, and the inclusion of several, early echoes greatly aids AIF calculation. In this approach, short EPI readouts allowed both gradient and spin echoes to be acquired in each excitation, without penalty in TE or slice coverage, and with the image quality benefits of multi-shot EPI. CBV maps may be generated from both GRE and SE timecourses. Simultaneous R2 and R2* mapping also helps to tackle the longstanding problem of dynamic and static dephasing components and is a logical next step towards quantitative DSC.

References. [1]Newbould R, *et al*. 14th ISMRM,2006,673. [2]Kiselev V, *et al*. MRM 2005:53:553-563. [3]Donohue, *et al*. MRM 43:845–853,2000. [4]Schmainda, *et al*. AJNR 25:1524-1532,2004. [5]Rausch M, *et al*. MRI 18:1235-1243,2000. [6]Ostergaard L, *et al*. MRM 36:715-25,1996.

Acknowledgements. This work was supported in part by the NIH (1R01EB002711), the Center of Advanced MR Technology at Stanford (P41RR09784), Lucas Foundation, and Oak Foundation.